Changes in Reference Evapotranspiration over Southwest China during 1960–2018: Attributions and Implications for Drought

Zhaoqi Zeng [1,2], Wenxiang Wu [1,3,*], Yang Zhou [1], Zhaolei Li [4], Mei Hou [1] and Han Huang [5]

[1] Key Laboratory of Land Surface Pattern and Simulation, Institute of Geographic Sciences and Natural Resources Research, Chinese Academy of Sciences, Beijing 100101, China; zengzhaoqi24@icloud.com (Z.Z.); zhouyang@igsnrr.ac.cn (Y.Z.); wangziyi17@mails.ucas.edu.cn (M.H.)

[2] Department of Environment and Resources, University of Chinese Academy of Sciences, Beijing 100049, China

[3] CAS Center for Excellence in Tibetan Plateau Earth Sciences, Chinese Academy of Sciences (CAS), Beijing 100101, China

[4] National Engineering Laboratory for Efficient Utilization of Soil and Fertilizer Resources, Key Laboratory of Agricultural Environment in Universities of Shandong, College of Resources and Environment, Shandong Agricultural University, Taian 271018, China; lizlei@igsnrr.ac.cn

[5] School of Land Science and Technology, China University of Geosciences, Beijing 100083, China; wuwenxiang68@sina.com

* Correspondence: wuwx@igsnrr.ac.cn

Abstract: Reference evapotranspiration (ET_0) is important to the global energy balance and to hydrological cycling. However, the extent to which ET_0 changes, the main driving factors, and especially the implications of its shift for drought in Southwest China are not clear. In this study, trends in Penman–Monteith ET_0 and other climatic parameters at 79 stations in Southwest China from 1960 to 2018 were investigated by using the Mann–Kendall test. Furthermore, partial correlation analysis and multiple linear regression were used to determine the dominant climate driving factors in changes in ET_0. The relative contribution of precipitation and ET_0 to drought duration was also quantified based on spatial multiple linear regression. Results revealed that annual ET_0 decreased significantly ($p < 0.01$) at a rate of 14.1 mm per decade from 1960 to 2000, and this decrease disappeared around 2000. For the entire study period, the sunshine duration (Tsun) was the most closely correlated with and played a dominant role in the variations in ET_0 at both annual and seasonal (summer and autumn) timescales, whereas the relative humidity was the most dominant factor in the spring and winter. Trends in the Standardized Precipitation Evapotranspiration Index revealed that drought has become more serious in Southwest China, and ET_0 has made a greater contribution to the duration of drought than precipitation. Our findings highlight that more attention should be paid to the impacts of ET_0 changes on drought in Southwest China. Furthermore, these results can provide a reference for the allocation of water resources and the implementation of countermeasures to climate change.

Keywords: climatic parameters; reference evapotranspiration; dominant factors; drought duration; Southwest China

1. Introduction

Climate change, which is associated with increasing greenhouse gas emissions, has led to the profound concern that future water availability may be threatened [1]. As the global surface temperature increases, the water-holding capacity and water vapor transport of the atmosphere may

increase, which will further accelerate the hydrological cycles and increase evapotranspiration [2]. Evapotranspiration, as an essential component of the hydrological cycle and the most important climatic element, controls energy and water exchange in the boundary layer [3]. Its variations will have a large effect on ecosystem stability, the water–energy cycle, the occurrence of drought, water resources management, and human activities [4]. However, because of the complex interactions among the components of the land–plant–atmosphere system, the actual evapotranspiration is very difficult to measure directly on a wide scale. Therefore, it is commonly estimated from weather data (sunshine duration, wind speed, temperature, and relative humidity) by using the Penman–Monteith method [5] to derive the so-called reference evapotranspiration (ET_0), which is usually the basis for the actual evapotranspiration [6]. Variation in ET_0 is a consequence of variations in all meteorological factors and very susceptible to land-use change [7], and can be seen as the most excellent indicator for the activities of humans, climate change, and the water cycle. Therefore, analyzing the variation in ET_0 has been widely applied as a valuable reference to assess ecological changes and agricultural water requirements.

In the past 100 years, the mean land surface air temperature has increased by 0.74 °C globally and by 0.5–0.8 °C in China [8]. However, unlike the general expectation that a warmer climate will bring about an increase in ET_0, several studies have demonstrated that ET_0 has shown a steady downward trend over the past decades, both globally [9] and in many regions of the world [10–13]. In China, a decreasing ET_0 has also been observed in Southwest China [14], Northwest China [15], the Tibetan Plateau [16], the Loess Plateau [17], the three-river source region of China [18], the Yellow River Basin [19], the Haihe River Basin [20], and throughout the country [21]. This is known as the "evaporation paradox" phenomenon [9]. However, a number of studies have also pointed out an increasing trend in ET_0 in some regions of China [22,23]. Even in areas with a decreasing trend in ET_0 in the past, the evaporation paradox phenomenon has disappeared in recent decades because of the continual change in climate [24,25]. To illuminate the complexity of the intersection among various meteorological factors and eventually understand the underlying mechanisms for the changed ET_0 in different regions and at different time periods, numerous methods (e.g., statistical methods, sensitivity analysis, and contribution rate analysis) have been applied to distinguish among the main driving forces causing changes in ET_0. For example, Han et al. [24] explored the impacts of meteorological factors on variations in ET_0 in Jing-Jin-Ji by using multiple regression analysis, and found that the annual ET_0 decreased significantly from 1961 through 1991, mainly because of the decrease in wind speed and the sunshine duration. However, they also found that a continually increasing air temperature had become the dominant factor contributing to the increase in ET_0 after 1992. Zhang et al. [26] used a sensitivity analysis and the linear regression method to determine the factors involved in the pan-evaporation of the Poyang Lake Basin. They found that a decrease in temperature from 1959 to 1973 and decreases in wind speed and solar radiation from 1974 to 1995 were mostly responsible for the pan-evaporation decrease; subsequently, an increase in pan-evaporation from 1996 to 2012 was mainly found to be due to significant increases in wind speed and air temperature. Most studies have carried out these works at yearly timescales. However, the change in ET_0 at seasonal timescales plays a more important role in agricultural production. In addition, several studies have also attempted to evaluated trends in evaporation and its component worldwide [27]. However, because of the complex interactions among various meteorological factors involved in ET_0, no general conclusions have been drawn; thus, explaining the trends in ET_0 remains challenging throughout the world.

Furthermore, accelerated hydrological cycles accompanied by frequency hydrological events (such as drought, floods, and extreme precipitation anomalies) have also recently become the focus of studies on both regional and even global hydroclimatic changes [28–30]. It is worth noting that changes in patterns of precipitation and evaporation with continuing global warming are expected to result in drought events of greater magnitude, frequency, and duration [31]. Most articles in the literature have mainly attempted to explain the mechanism of the continuous increase in drought events from the close relationship between precipitation and drought [32,33], whereas the impacts of ET_0 have been

given less attention. However, recent research has emphasized that the contribution of ET_0 to drought could be equivalent to, or even higher than, that from precipitation [34–36]. Therefore, it is essential to conduct regional research to quantify the relative contribution of ET_0 to drought anomalies.

Southwest China, one of the main grain-producing areas, provides approximately 16% of the national food supply and is located mainly in a humid area. Traditionally, it has been widely believed that the southwestern region is rich in rainfall and has a large amount of water resources; thus, the serious drought problem in agriculture is often overlooked. Especially in recent years, Southwest China has suffered great losses from extremely severe drought. For example, the severe drought that occurred in 2006 caused a shortage of drinking water for more than 16 million people and 17 million livestock [37]. Another extreme drought event that occurred in 2010 was considered a "once-in-a-century" drought. It devastated crops across more than 4 million hectares of farmland, causing 25% of the areas to yield no harvest [38]. In addition, Southwest China has a large deficiency in available water and thus faces a severe water shortage crisis, mainly because of the uneven distribution of water resources. The water-rich areas and month in which precipitation is concentrated do not match the water demand areas and times of agricultural water demand [39]. Agricultural irrigation is the largest water-consuming sector in Southwest China. Data from 2000 to 2008 show that agricultural water consumption accounts for more than 60% of the total water consumption in the region. However, rapid industrialization and urbanization have induced a large proportion of the irrigation water to flow to industrial and other sectors, which further strains the water available for agriculture and causes enormous food security pressure. By considering the importance of ET_0 to estimate the water demand for crops and drought forecasting systems [40], in-depth study of the spatial–temporal variations in ET_0 will allow researchers to better understand climate change and hydroclimatological extremes (e.g., droughts) and develop appropriate strategies to sustain regional development (e.g., water resources and agriculture).

Therefore, the main objectives of this study were as follows: (1) To detect the spatial and temporal variation in ET_0 and climatic driving factors in Southwest China from 1960 to 2018, (2) to investigate annual and seasonal trends in ET_0, (3) to determine the dominant factors inducing changes in ET_0, and (4) to identify the relative contributions of precipitation and ET_0 to the duration of drought.

2. Data and Methods

2.1. Study Area and Materials

Southwest China is located between 21–34° N and 97–110° E and mainly consists of three provinces, Yunnan, Sichuan, and Guizhou, and a municipality, Chongqing. It is also one of the most densely populated regions in China, accounting for about one-sixth of the total national population. The area is dominated by a subtropical monsoon climate with the characteristics of a dry winter and wet summer (the mean precipitation from April to October constitutes more than 85% of the total) [41]. The average annual temperature is 14–24 °C in most areas, and the average annual precipitation is more than 900 mm.

The high-quality data used in this study were mainly climatic data collected from 1960 to 2018 in Southwest China, including the monthly mean temperature (°C), relative humidity (%), sunshine duration (h), and wind speed at 10 m (m/s) at 79 weather stations. The climatic data were provided by the China Meteorological Administration (http://data.cma.cn). The locations of these weather stations in Southwest China are shown in Figure 1. The quality of meteorological data was examined, and the occasional missing data (no more than 1% of the total data) were replaced by average data for the same month in the neighboring years.
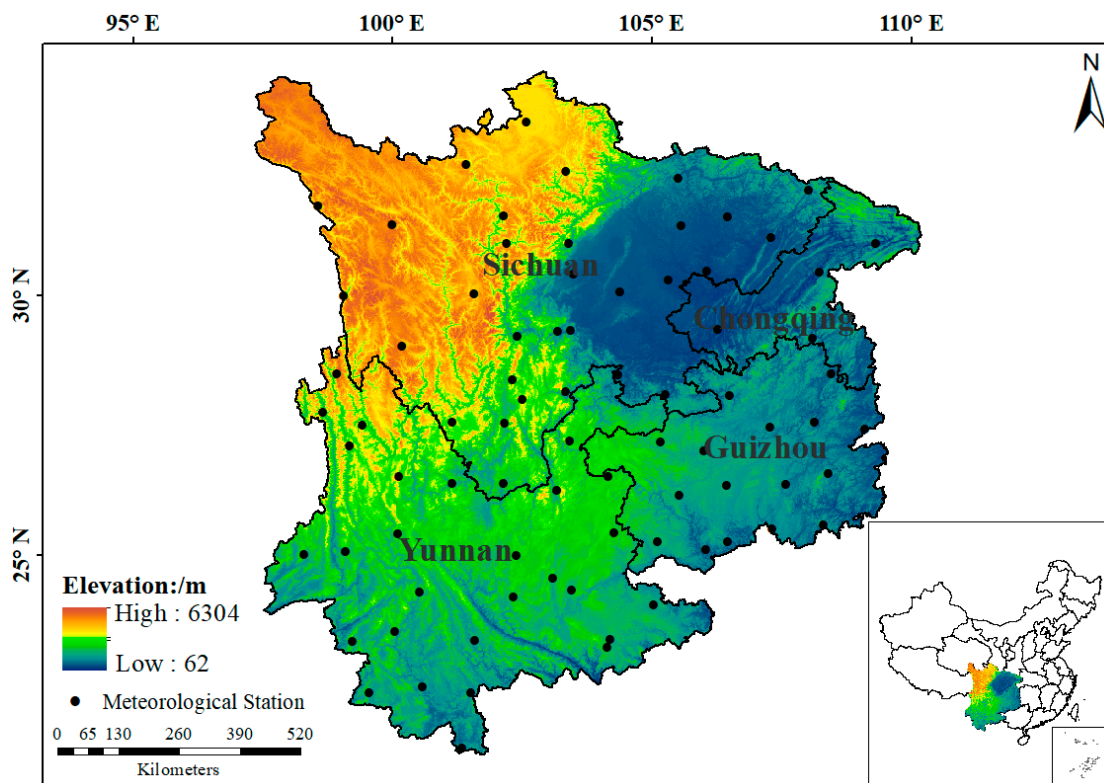
Figure 1. Locations of rain-gauge stations in Southwest China.

2.2. Method of Calculating ET$_0$

The Penman–Monteith equation was selected to calculate ET$_0$ in this work, as recommended by the Food and Agriculture Organization of the United Nations in 1998 [5]. The model integrates the mass transfer and energy balance, while considering the physiological characteristics of vegetation valid in both humid and arid climates, and is thus widely used around the world. The following equation was used to calculate ET$_0$ at the 79 observation stations:

$$\text{ET}_0 = \frac{0.408\Delta(R_n - G) + \gamma\left(\frac{900}{T_{\text{mean}}+273}\right)U_2(e_s - e_a)}{\Delta + \gamma(1 + 0.34U_2)} \tag{1}$$

where ET$_0$ is the evapotranspiration rate from a reference surface (crop or grass), not short of water, called the reference crop evapotranspiration or reference evapotranspiration; R_n is the net radiation at the reference crop surface [MJ·m−2·day−1]; G is the soil heat flux density [MJ·m−2·day−1]; T_{mean} is the mean air temperature at a height of 2 m [°C]; U_2 is the wind speed at a height of 2 m [m·s−1]; e_s is the saturation water vapor pressure [kPa]; e_a is the actual water vapor pressure [kPa]; Δ is the slope of the vapor pressure curve [kPa·°C−1]; and γ is the psychometric constant [kPa·°C−1]. The net radiation was estimated by using the sunshine hours and the maximum and minimum air temperature data. Detailed equations for R_n, G, e_s, Δ, and γ can be found in the study by Allen et al. [5]. Note that all the computations in this study were performed on a monthly scale.

2.3. The Mann–Kendall Test for Trend Analysis

We investigated the trends in ET$_0$ by using the Mann–Kendall method [42,43]. The Mann–Kendall test is a rank-based nonparametric method for assessing the significance of a trend, and it has been widely used for the analysis of hydrologic and meteorological trends [44,45]. Because the Mann–Kendall method does not require any assumptions for the distribution of data, it is highly recommended

for general use by the World Meteorological Organization. The following procedures were used to calculate the statistical value S and the standardized test statistic Z:

$$S = \sum_{i=1}^{n-1} \sum_{j=i+1}^{n} sgn\left(x_j - x_i\right) \tag{2}$$

where n is the number of observations, x_i and x_j are the values of years i and j in the time series, and

$$sgn\left(x_j - x_i\right) = \begin{cases} 1 & if \left(x_j - x_i\right) > 0 \\ 0 & if \left(x_j - x_i\right) = 0 \\ -1 & if \left(x_j - x_i\right) < 0 \end{cases} \tag{3}$$

$$Var(S) = \frac{n(n-1)(2n+5) - \sum_{i=1}^{m} t_i(t_i - 1)(2t_i + 5)}{18} \tag{4}$$

where m is the number of tied groups, t_i is the number of data values in the pth group, and

$$= \begin{cases} \frac{S-1}{\sqrt{Var(S)}} & if \ S > 0 \\ 0 & if \ S = 0 \\ \frac{S+1}{\sqrt{Var(S)}} & if \ S < 0 \end{cases} \tag{5}$$

where the Z value is used to evaluate the statistical trend of the time series data, such that if Z < 0, the data show a decreasing trend, and vice versa. If $|Z| > Z_{(1-a/2)}$, the null hypothesis is rejected at a given confidence level a. In other words, there is a significant trend in the time series data. Critical Z values of ±1.64, ±1.96, ±2.58, and ±3.29 were used for the probabilities of a = 0.1, 0.05, 0.01, and 0.001, respectively.

2.4. Partial Correlation Analysis

Partial correlations are measures of the effect of an individual parameter on the variance of the predicted values when the effect of the other parameters has been eliminated. For example, $R_{xy,z}$ is the correlation between parts x and y while controlling for the possible influences of z, and it can be calculated by Equation (6) [46]. In this study, partial correlation analysis was used to examine the relationships between ET_0 and the climatic driving factors, with the understanding that the larger the partial correlation coefficient is, the more important that factor is for the changes in ET_0 [47]:

$$R_{xy,z} = \frac{R_{xy} - R_{xz}R_{yz}}{\sqrt{\left(1 - R_{xz}^2\right)\left(1 - R_{yz}^2\right)}}, \tag{6}$$

2.5. Multiple Linear Regression

To evaluate the relative contribution rate of climatic driving factors to the variation in ET_0 in this study, multiple regression analysis was performed on a series of meteorological variables to establish a multiple linear regression equation. The relative contribution rate of the change in a variable to ET_0 was defined as the proportion of the regression coefficient of one variable that accounts for the sum of the regression coefficients of all the variables. The detailed calculation equations are as follows:

$$Y_S = aX_{1S} + bX_{2S} + cX_{3S} + \dots, \tag{7}$$

$$n_1 = \frac{|a|}{|a| + |b| + |c| + \dots}, \tag{8}$$

where Y_S is the standardized value of ET_0; X_{1S}, X_{2S}, X_{3S} ... are standardized values of the first meteorological factor, the second meteorological factor, the third meteorological factor, and so forth; a, b, c ... are regression coefficients for the first meteorological factor, the second meteorological factor, the third meteorological factor, and so forth; and n_1 is the relative contribution of the variation of X_{1S} to ET_0.

2.6. Relative Contribution of ET_0 to the Drought Duration in Southwest China

To calculate the relative contribution of ET_0 to the drought duration in Southwest China, a new drought index, the Standardized Precipitation Evapotranspiration Index (SPEI), was selected to quantify the drought. The SPEI was proposed by Vicente-Serrano et al. [48] and was calculated based on the difference between precipitation and ET_0 to describe the degree of deviation in regional dry and wet conditions from climatological mean conditions. It reveals that a decreasing SPEI may be caused by an abnormal decrease in precipitation or an increase in ET_0. The more negative the SPEI value, the more severe the drought. In addition, the main advantage of SPEI is that it can be calculated on different time-scales, and the different SPEI has different implications. For example, the SPEI at longer timescales (12 to 24 months) can reflect medium-term trends in precipitation and ET_0 patterns and may provide an annual estimation of the stream flows, reservoir levels, and even groundwater levels; at shorter timescales (l to 3 months), the SPEI can mirror prompt changes in soil moisture, which is particularly important for food production [49]. A detailed calculation of this method can be found in the references of Vicente-Serrano et al. [48]. In this study, the SPEI was calculated at 3-month (for drought duration and drought frequency analysis) and 12-month (for drought trend analysis) time scales, respectively, according to Yu et al. [37]. According to the results of the SPEI at a 3-month timescale, the drought duration was defined as the longest number of consecutive months with an SPEI of less than −0.5; the drought frequency with a specific drought severity (SPEI < −0.5) was calculated as the ratio of the drought occurrences to the total drought or wet (SPEI > 0) occurrences. Furthermore, spatial multiple linear regression was carried out to quantify the relative contributions of precipitation and ET_0 to the drought duration, with precipitation and ET_0 as the independent variables and the drought duration as the dependent variable for all of Southwest China.

3. Results

3.1. Spatial and Temporal Evolution of ET_0 and Climatic Factors

In this study, we analyzed the time variations and spatial distribution characteristics of ET_0 and five meteorological factors, namely, temperature (Tmean), relative humidity, wind speed (U2), sunshine duration (Tsun), and precipitation (Pre), over Southwest China from 1960 to 2018. Figure 2 shows the annual variations in ET_0 and the five meteorological factors over the study period.

During the period from 1960 to 2000, the annual ET_0 decreased significantly ($p < 0.01$), by 14.1 mm per decade, but an obvious increase occurred after 2000, especially during the period from 2001 to 2013, when the annual ET_0 increased significantly ($p < 0.01$) by 51.3 mm per decade. For the entire study time series from 1960 to 2018, a statistically nonsignificant ($p > 0.05$) increase in the annual ET_0 of 9.7 mm per decade was found. The air temperature, including Tmean, Tmax, and Tmin, all showed a significantly ($p < 0.01$) increasing trend over the entire study period. Relative humidity declined over the entire period by −0.44% per decade, and the value of the Mann–Kendall trend test reached −3.67 ($p < 0.01$). The average wind speed from the 79 stations showed a −0.02 m/s per decade decline during the period from 1960 to 2018 and the decreasing trend was significant, whereas the Z value of the Mann–Kendall trend test was −2.66 ($p < 0.01$). During the same period, the Tsun showed a significant decrease by −27.4 h per decade, and the Z value reached −4.34 ($p < 0.01$). In addition, precipitation showed a nonsignificant decreasing trend at the rate of 2.41 mm per decade, and the Z value was −0.56 ($p > 0.05$).
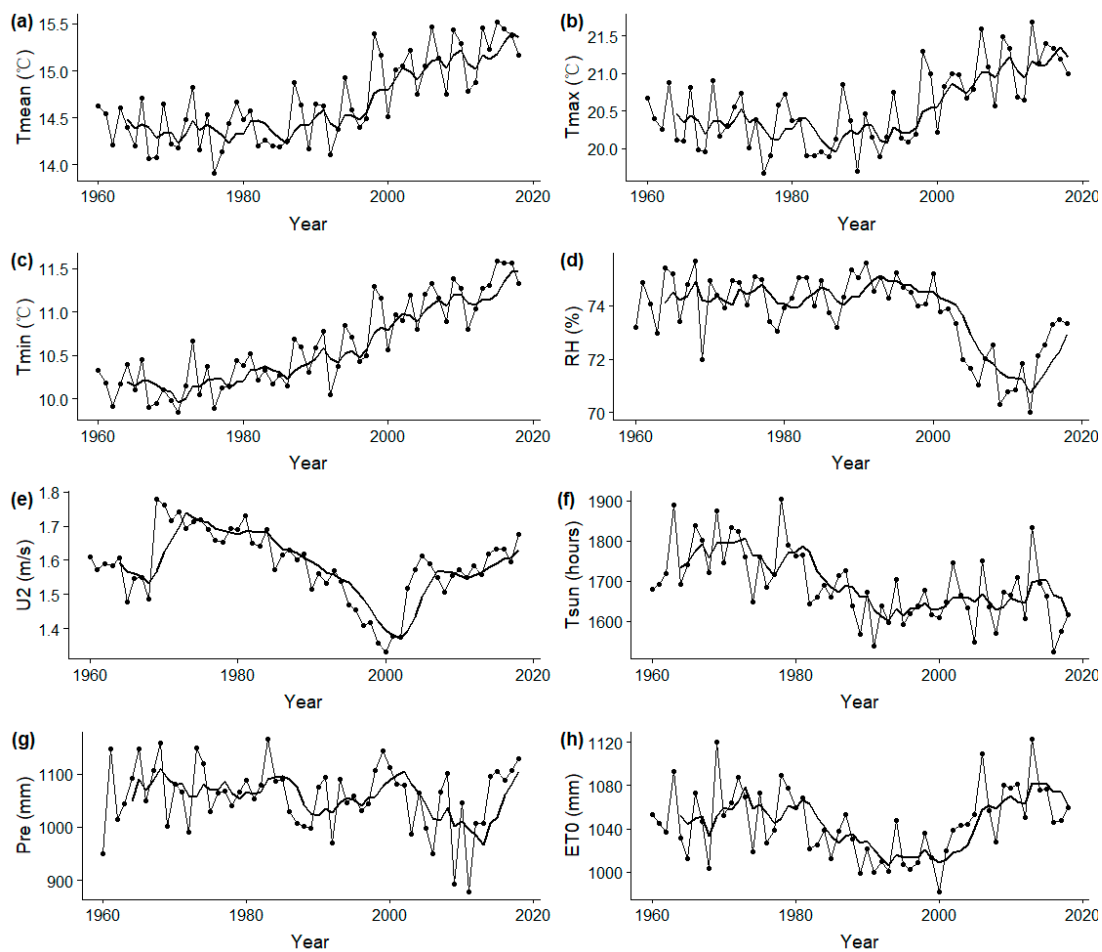
Figure 2. Annual average and 5-year moving average (**a**) air temperature (Tmean), (**b**) maximum temperature (Tmax), (**c**) minimum temperature (Tmin), (**d**) relative humidity (RH), (**e**) wind speed (U2), (**f**) sunshine hours (Tsun), (**g**) precipitation (Pre), and (**h**) reference evapotranspiration (ET$_0$) of the Southwest China region from 1960 to 2018.

The spatial distributions of ET$_0$ and the five climatic factors are illustrated in Figure 3. The results show that the areas of high temperature were located mainly in southwestern Yunnan, with the average maximum temperature (Tmax) reaching 30.7 °C (Figure 3b). The low-temperature areas were located mainly in northwestern Sichuan, with the average minimum temperature (Tmin) reaching −4.9 °C (Figure 3c). The spatial distribution characteristics of relative humidity were somewhat similar to the spatial distribution of Tmean (Figure 3a,d), with the values declining from the southeast to the northwest of the study area. Additionally, the areas of high sunshine duration were located mainly in the eastern part of Southwest China, including Yunnan and eastern Sichuan (Figure 3e). With respect to the wind speed in Southwest China, it reached maximum values of 3.16 m/s in northeastern Yunnan and southwestern Sichuan, whereas in Chongqing and southwestern Yunnan, the wind speed was about 1 m/s (Figure 3f). When calculated mainly by these four meteorological factors, the spatial distribution of ET$_0$ was somewhat similar to that of Tsun, with the areas of high ET$_0$ located mainly in Yunnan and southwestern Sichuan (Figure 3h). The maximum values of ET$_0$ in these areas reached 1678 mm year^{-1}. Additionally, the high-precipitation areas were located mainly in southwestern Yunnan, where the maximum values reached 2228.9 mm year^{-1} (Figure 3g).
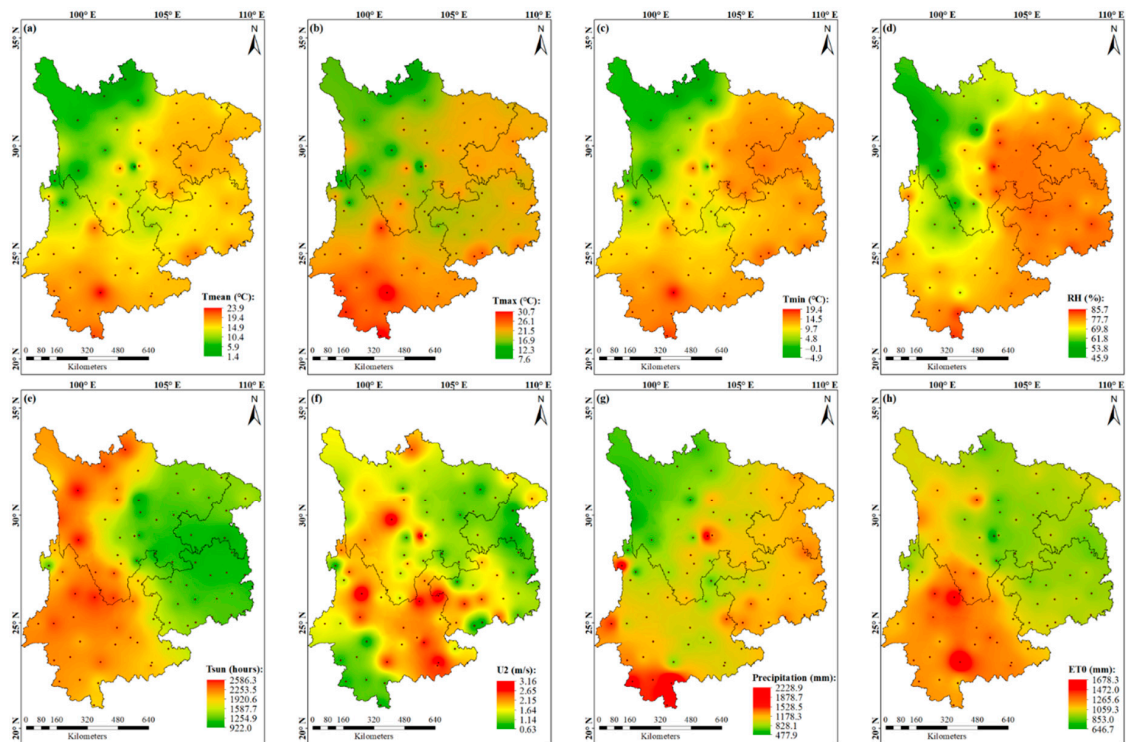
Figure 3. Spatial distribution of annual ET$_0$ (h) and climatic factors, including (**a**) mean air temperature (Tmean), (**b**) maximum temperature (Tmax), (**c**) minimum temperature (Tmin), (**d**) relative humidity (RH), (**e**) sunshine hours (Tsun), (**f**) wind speed (U2), (**g**) precipitation, and (**h**) reference evapotranspiration (ET$_0$).

3.2. Spatial Distribution of Trends in ET$_0$ and Climatic Factors

Temperature, wind speed, relative humidity, and sunshine duration are the four main driving factors that affect changes in ET$_0$. Figure 4 shows the results of the changing trends for these four factors for each of the 79 ground stations from 1960 to 2018. As shown in Figure 4a, a significantly increasing trend for annual Tmean occurred in 68 of the 79 stations, and these stations were located over all areas of Southwest China. With respect to the wind speed (U2), the majority of stations (64.6%) showed a decreasing trend (Figure 4b). Among them, the number of stations registering a significantly decreasing trend reached 30, and these stations were located mainly in the middle area. In addition, 13 stations showed a significantly increasing trend, and these were scattered in patches in Southwest China. Furthermore, the greatest proportion of stations showed a significantly decreasing trend in relative humidity (53.2%) and sunshine duration (62%); these stations covered almost all of the study area (Figure 4c,d). Only four stations showed a significantly increasing trend in sunshine duration, and these were located mainly in southwestern Yunnan (Figure 4d).
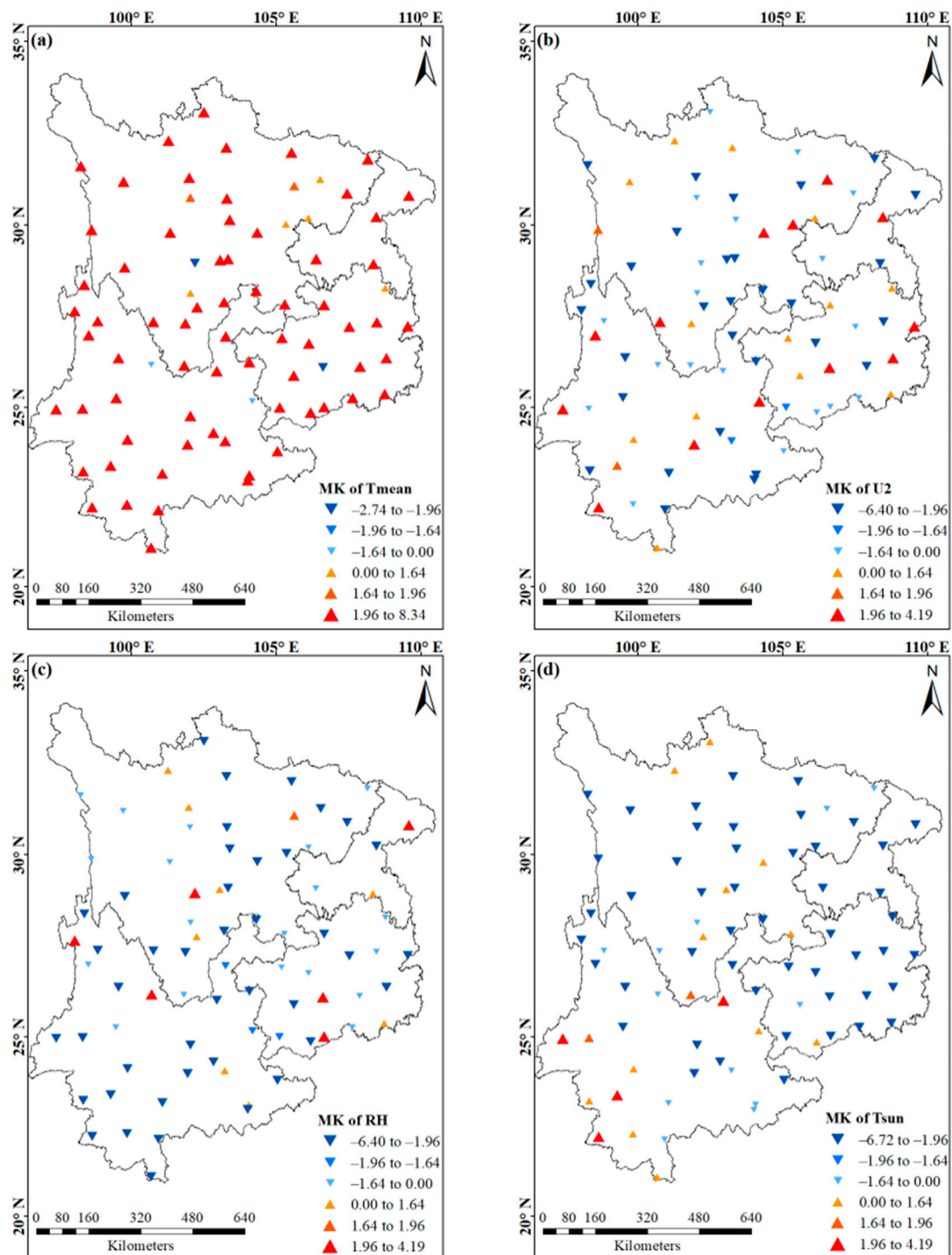
Figure 4. Spatial pattern trends in climatic driving factors of ET_0 from 1960 to 2018: (**a**) Mean air temperature (Tmean), (**b**) wind speed (U2), (**c**) relative humidity (RH), and (**d**) sunshine hours (Tsun). Triangles of different sizes indicate trends of different magnitudes. MK, Mann–Kendall test.

Figure 5 shows the results of changing trends on the annual and seasonal ET_0 for each of the stations from 1960 to 2018. As illustrated in Figure 5a, the stations that showed an increasing trend for annual ET_0 accounted for 50.6% of the total. Among them, 16 stations showed a significantly increasing trend, with a maximum increase of 3.45 mm year^{-1}, and these stations were located mainly in eastern Yunnan and northern Sichuan. During the same period and at the same annual timescale, the stations that showed a significantly decreasing trend in ET_0 were located mainly in Guizhou.

Overall, the spatial distribution of annual ET_0 trend change was more consistent to the distribution of annual Tsun trend (Figure 4d, Figure 5a), which indicates that Tsun may be the dominant meteorological factor for ET_0 change in southwest China. In addition, the changes in ET_0 at seasonal timescales plays a more important role in agricultural production, and thus the changes in ET_0 in different seasons were also provided in Figure 5b–e. In the spring (Figure 5b), 44 stations showed an increasing trend, at the rate of 0.01–0.88 mm year^{-1}. Among them, six stations located mainly in northeastern Sichuan and eastern Guizhou showed a significantly increasing trend. Furthermore, a significantly decreasing trend for ET_0 in the spring occurred at 14 of the 35 stations, and these were scattered in patches in Southwest China. In the summer, the number of the stations that showed a significantly increasing trend increased to 12 compared with the spring, and these stations were located mainly in southwestern and northeastern Yunnan (Figure 5c). It is worth mentioning that nearly all of the stations in Guizhou and Chongqing displayed a decreasing trend in the summer. In the autumn and winter, the areas where ET_0 showed an increasing trend increased significantly compared with the spring and summer. The number of stations that exhibited a significantly increasing trend increased to 21 in the autumn and 17 in the winter, and these stations were located mainly in Yunnan and Sichuan. The increasing rate ranged from 0.01 to 0.83 mm year^{-1} in the autumn and 0.03 to 0.93 mm year^{-1} in the winter (Figure 5d,e). Furthermore, only four and five stations displayed a significantly decreasing trend in the autumn and winter, respectively. These stations were located mainly in central and southern Guizhou and southeastern Chongqing.
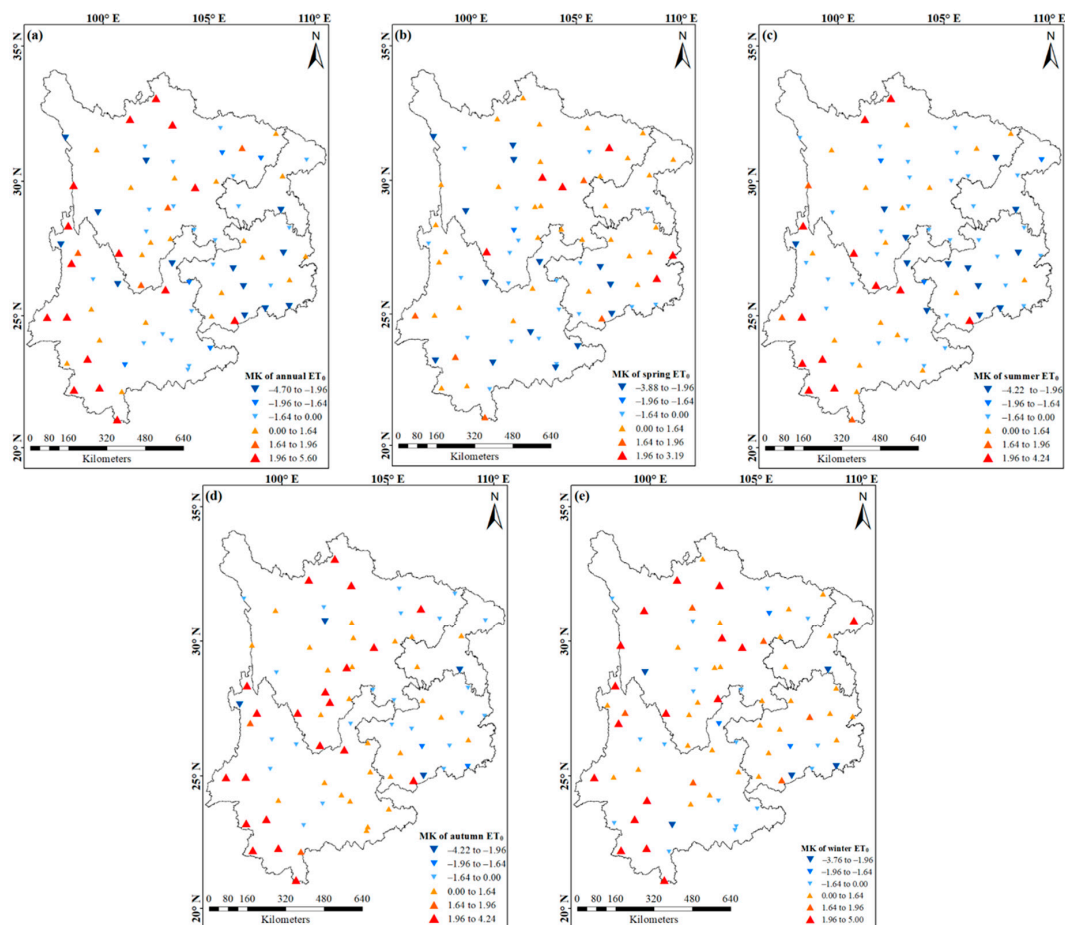

Figure 5. Spatial distribution of annual and seasonal trends in ET_0 from 1960 to 2018: (**a**) Annual ET_0, (**b**) spring ET_0, (**c**) summer ET_0, (**d**) autumn ET_0, and (**e**) winter ET_0. Triangles of different sizes indicate trends of different magnitudes. MK, Mann–Kendall test.

3.3. Relationships between ET_0 and Other Climatic Factors

The ET_0 was affected by several climatic factors and interactions among them. To gain a better understanding of the relationships between ET_0 and the climatic driving factors (Tmean, U2, relative humidity, and Tsun), the partial correlation method was appropriate because it can identify the "real" correlation between ET_0 and a specific factor by eliminating the influences of all other factors. The results show that ET_0 was negatively correlated with relative humidity but positively correlated with mean air temperature, wind speed, and sunshine duration (Table 1) for all stations at the annual timescale. These results are consistent with our knowledge that greater relative humidity will lead to a decrease in ET_0 but that increased temperature, wind speed, and sunshine duration will cause an increase in ET_0.

Table 1. Partial correlation between reference evapotranspiration (ET_0) and other meteorological factors for different periods.

Period	Timescale	Mean Air Temperature (Tmean)	Wind Speed (U2)	Relative Humidity (RH)	Sunshine Duration (Tsun)
1960–2018	Yearly	0.83	0.90	−0.84	0.95
1960–2018	Spring	0.90	0.95	−0.95	0.96
1960–2018	Summer	0.90	0.83	−0.91	0.99
1960–2018	Autumn	0.82	0.78	−0.70	0.90
1960–2018	Winter	0.92	0.92	−0.90	0.83
1960–2000	Yearly	0.80	0.88	−0.56	0.93
2001–2018	Yearly	0.76	0.87	−0.88	0.93

All data are statistically significant at 1% confidence level ($p < 0.01$).

For the entire area of Southwest China, we found that ET_0 was the most closely correlated with a change in Tsun, followed by U2, relative humidity, and Tmean, with correlation coefficients of 0.95, 0.9, −0.84, and 0.83, respectively. In addition, the degree of correlation between ET_0 and other meteorological driving factors was slightly different in each season. For example, ET_0 was most closely correlated with Tsun in the spring, summer, and autumn, with correlation coefficients of 0.96, 0.99, and 0.90, respectively. However, in winter, ET_0 was most closely correlated with Tmean and U2 (0.92) and least closely correlated with Tsun (0.83). Because ET_0 showed a decreasing trend from 1960 to 2000 and an increasing trend after 2000, we also explored the correlation between ET_0 and other driving climatic factors in two time periods, 1960–2000 and 2001–2018. The results showed that Tsun was also the most closely correlated factor in both 1960–2000 and 2001–2018, with the same correlation coefficient, 0.93. Additionally, the correlation coefficients between ET_0 and U2 changed slightly from the time period of 1960–2000 (0.88) to 2001–2018 (0.87). However, a stronger correlation was found between ET_0 and relative humidity from 2001 to 2018 (−0.88) than from 1960 to 2000 (−0.56), whereas the correlation coefficients between ET_0 and Tmean were lower from 2001 to 2018 (−0.88) than from 1960 to 2000 (−0.56). These results demonstrate that changes in the trend for ET_0 in 2000 may be related to Tmean and relative humidity.

3.4. Quantitative Estimation of the Influence of Climatic Factors on Changes in ET_0

A differential method was used to identify the combined influences of the meteorological variables on ET_0 and eventually attribute the change in ET_0 to them. Table 2 lists the annual and seasonal evaluation results of the combined relationship between ET_0 and all climatic driving factors, based on the multiple linear regression method, as well as the contributions of the four primary meteorological variables to the changes in ET_0 from 1960 to 2018.

Table 2. Correlation coefficients and rate of relative contributions to ET_0 among the factors driving climate change.

Timescale	Meteorological Factor	Regression Coefficients	Relative Contribution	Influence Degree Sort	Significance Level
Yearly	Mean air temperature (Tmean)	0.370	23.36	Tsun > Tmean > RH > U2	$R^2 = 0.975$ $p < 0.01$
	Wind speed (U2)	0.372	22.49		
	Relative humidity (RH)	−0.374	22.63		
	Sunshine duration (Tsun)	0.538	32.52		
Spring	Mean air temperature (Tmean)	0.282	20.38	RH > Tsun > U2 > Tmean	$R^2 = 0.993$ $p < 0.01$
	Wind speed (U2)	0.335	24.18		
	Relative humidity (RH)	−0.387	27.94		
	Sunshine duration (Tsun)	0.381	27.50		
Summer	Mean air temperature (Tmean)	0.215	16.24	Tsun > RH > Tmean > U2	$R^2 = 0.994$ $p < 0.01$
	Wind speed (U2)	0.128	9.16		
	Relative humidity (RH)	−0.254	19.15		
	Sunshine duration (Tsun)	0.730	55.01		
Autumn	Mean air temperature (Tmean)	0.408	25.05	Tsun > Tmean > U2 > RH	$R^2 = 0.935$ $p < 0.01$
	Wind speed (U2)	0.333	20.45		
	Relative humidity (RH)	−0.303	18.60		
	Sunshine duration (Tsun)	0.585	35.90		
Winter	Mean air temperature (Tmean)	0.399	27.42	RH > Tmean > U2 > Tsun	$R^2 = 0.980$ $p < 0.01$
	Wind speed (U2)	0.369	25.39		
	Relative humidity (RH)	−0.414	28.47		
	Sunshine duration (Tsun)	0.271	18.72		

At the annual timescale, the results show that the sunshine duration (33.52%) was the primary driving factor in changes in ET_0 from 1960 to 2018 in Southwest China, whereas the Tmean, U2, and relative humidity contributed almost equally, with relative contributions of 22.36%, 22.49%, and 22.63%, respectively. Although the significant decreases in Tsun and U2 had a decreasing effect on ET_0, this effect was offset by a significant increase in temperature and a decrease in relative humidity. The combined effects of the four climatic variables eventually resulted in a nonsignificant increase in ET_0.

Among the different seasons in the period from 1960 to 2018, the contribution rates of Tmean, U2, relative humidity, and Tsun were somewhat different. In the summer and winter, a significant decrease in Tsun was the most dominant factor contributing to the changes in ET_0, with relative contributions of 55.01% and 35.90%, respectively, in the two seasons. In the summer, however, Tsun exhibited strong control, causing a decreasing trend in ET_0. But in the autumn, the decreasing effect on ET_0 induced by a decrease in Tsun was offset by changes in temperature and relative humidity, eventually resulting in a nonsignificant increasing trend in ET_0. In the spring and winter, a significant decrease in relative humidity was found to be the predominant factor contributing to the changes in ET_0, with relative contributions of 27.94% and 28.47%, respectively, in the two seasons. A significant increase in Tmean also exacerbated the increase in ET_0 in the spring and winter, with relative contributions of 20.38% in the spring and 27.42% in the winter. In the spring, however, the increasing trend of ET_0 induced by relative humidity and Tmean was offset by the effects of a significant ($p < 0.01$) decrease in U2 and Tsun, with relative contributions of 24.18% and 27.50%,

respectively. In the winter, the contribution of U2 (25.39%) to changes in ET_0 was roughly similar to that in the spring, but the relative contribution of Tsun was lowest (18.72%) and showed a nonsignificant ($p > 0.05$) decreasing trend. These changes may be the main reason the upward trend in ET_0 was more obvious in the winter than in the spring.

3.5. Spatial Distribution of the Attribution of Changes in ET_0

Figure 6 shows the spatial pattern of the contribution of climatic factors to trends in ET_0 from 1960 to 2018 in Southwest China. The results show that the coefficients of the Tmean contribution were positive over most parts of Southwest China. Especially in the Sichuan Province, the significant increase in Tmean has made a greater contribution to the changes in ET_0 here compared with other regions. Regarding U2, Figure 6b illustrates that ET_0 levels in southwestern Yunnan and northwestern Sichuan were more sensitive to changes in U2 than those in Guizhou and Chongqing. Therefore, the high relative contribution of U2 may be one of the reasons for the significantly increasing trend in ET_0 in southwestern Yunnan. In addition, the contribution of relative humidity was relatively higher in regions located mainly in Guizhou, eastern Yunnan, and central and southeastern Sichuan (Figure 6c). It is worth mentioning that in most of these regions, the ET_0 showed a nonsignificant trend ($p > 0.05$). Furthermore, the spatial distribution of the contributions of Tsun was exactly the opposite of the distribution of Tmean, with the highest relative contributions in regions located mainly in Guizhou, Chongqing, southeastern Sichuan, and southwestern Yunnan (Figure 6d). In these regions in southwestern Yunnan, the difference was that Tsun showed a significantly increasing trend, compared with a decreasing trend in most other regions.
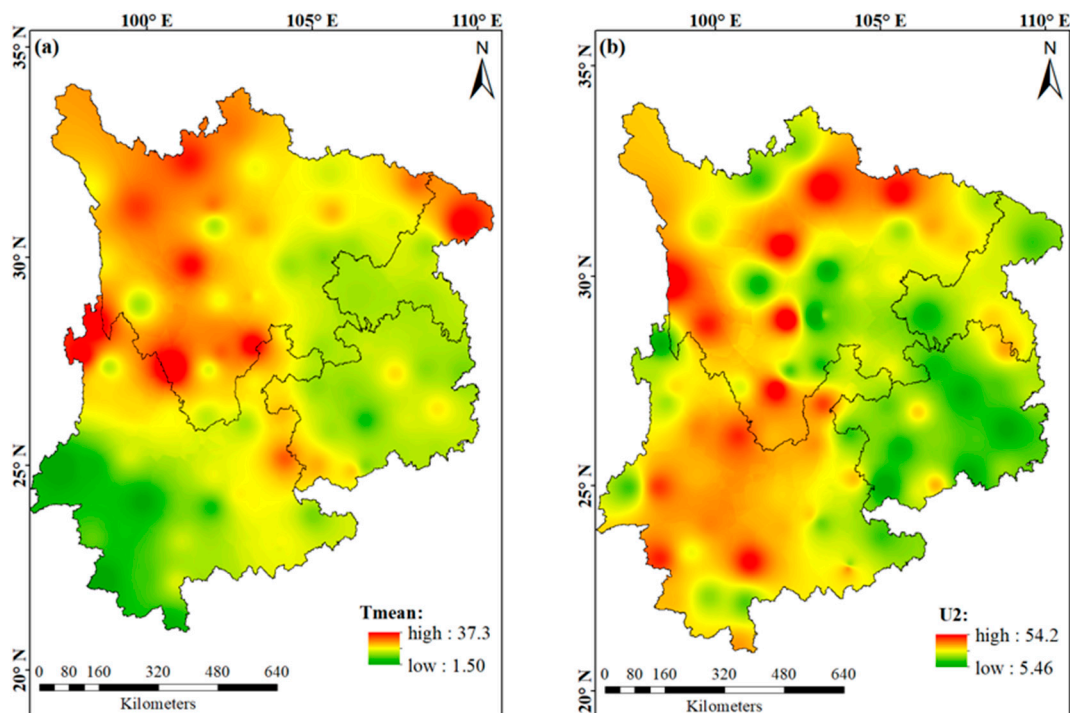

Figure 6. *Cont.*
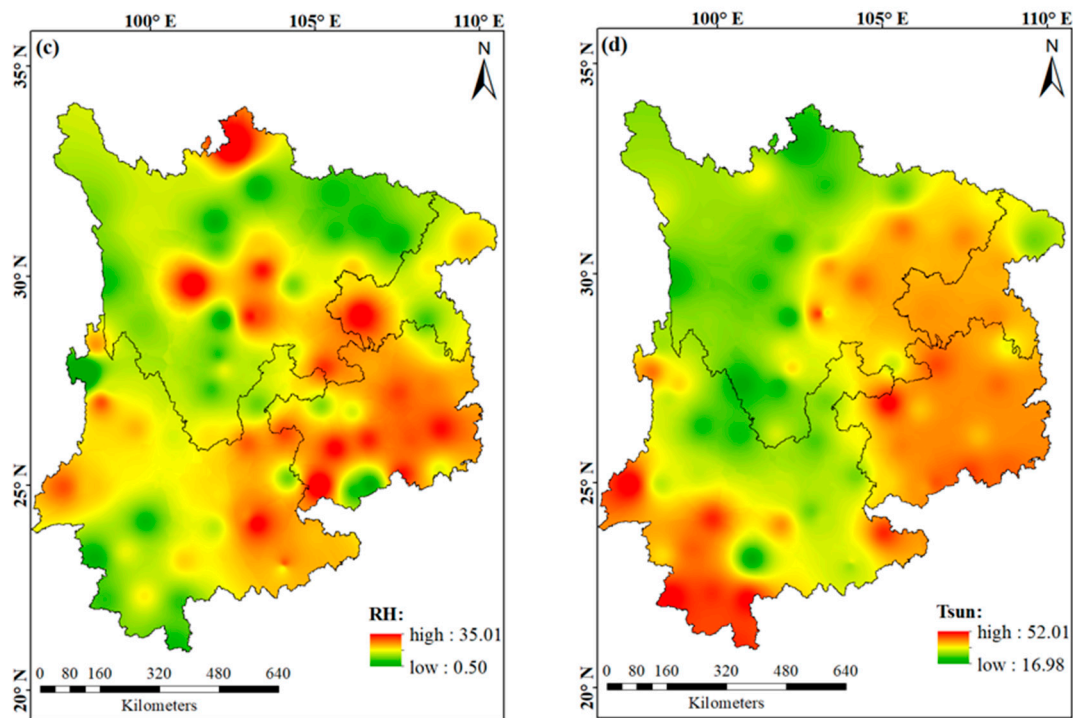
Figure 6. Spatial distribution of the relative contributions of key climatic driving factors for ET_0 from 1960 to 2018 in Southwest China: (**a**) Mean air temperature (Tmean), (**b**) wind speed (U2), (**c**) relative humidity (RH), and (**d**) sunshine hours (Tsun).

3.6. Relative Contribution of Precipitation and ET_0 to the Drought Duration in Southwest China

The drought duration is one of the most important characteristics of drought, and a long-term drought usually means that the drought is more severe. Southwest China has suffered great losses from long-term droughts that have begun occurring with greater frequency in recent years. We know that as the precipitation decreases and ET_0 increases, less water is available for storage in the soil, resulting in soil conditions favorable for drought evolution. However, less consideration has been paid to the contribution of ET_0 to duration of drought, and this contribution still remains disputed. To clarify the extent to which ET_0 changes contribute to drought duration in Southwest China, we firstly analyzed the temporal and spatial variations of drought trends (based on SPEI at 12-month timescale) from 1960 to 2018, as shown in Figures 7 and 8a, respectively. The results show that the annual SPEI decreased over the study period at a rate of 0.023 per decade. Especially after 2000, the decreasing precipitation and significantly increasing ET_0 both resulted in a significant decrease in the SPEI. The index reached its lowest values in 2010 (Figure 7). Spatially, the drying trends occurred at 53 of the 79 stations, and these stations were almost located over all areas in southwest China (Figure 8a).
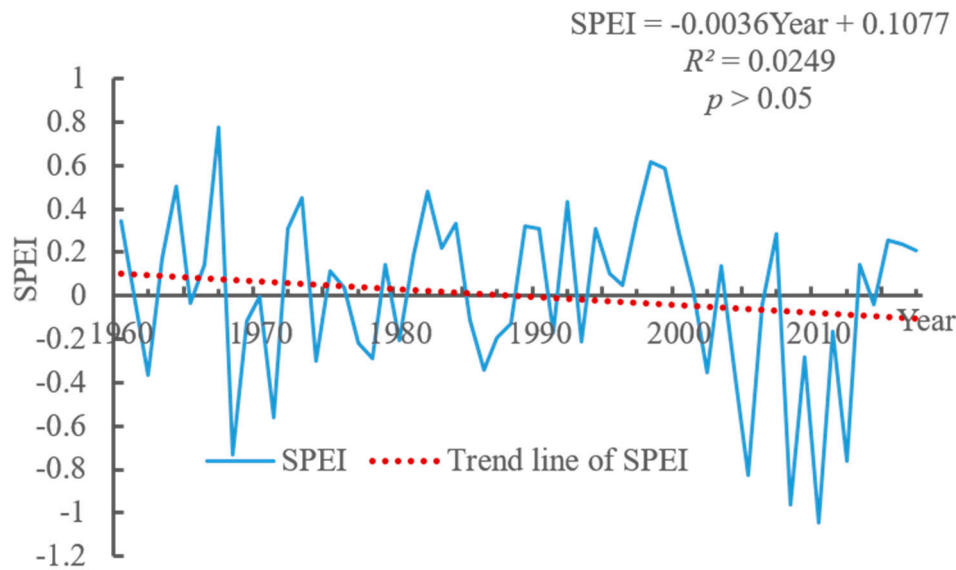
Figure 7. Time variations in the Standardized Precipitation Evapotranspiration Index (SPEI) from 1960 to 2018 in Southwest China.
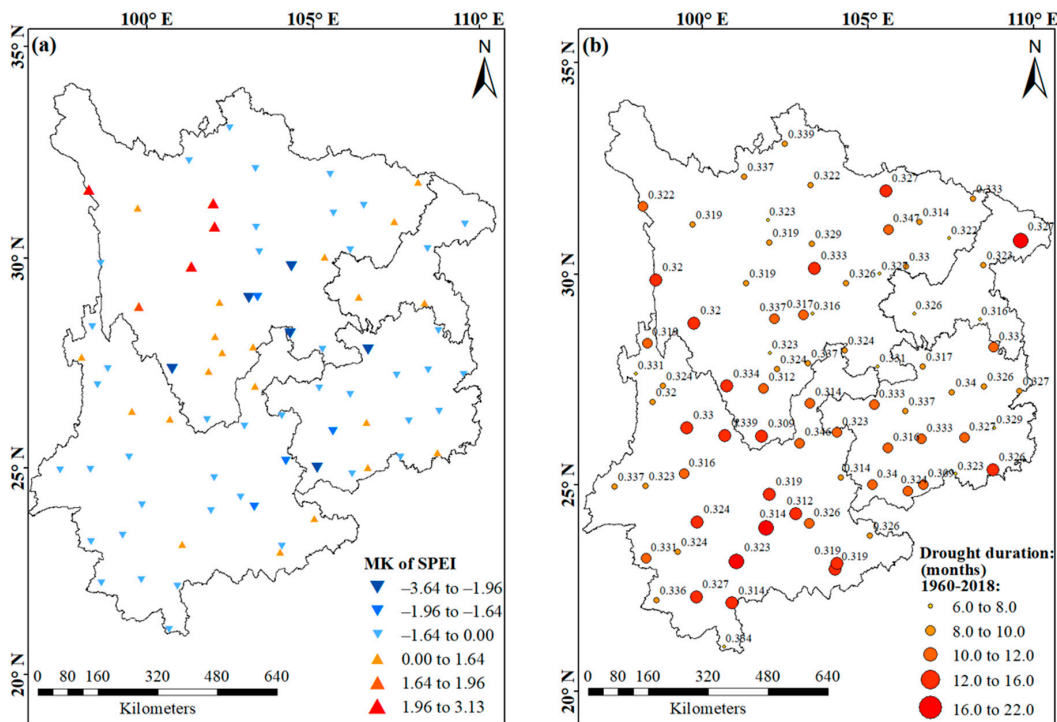

Figure 8. Spatial distribution of annual trends in SPEI (12-month timescales), drought duration, and frequency (identified by SPEI at 3-month timescale) from 1960 to 2018 in Southwest China: (**a**) Trends in SPEI; (**b**) drought duration and frequency (the numbers show drought frequency). MK, Mann–Kendall test.

Furthermore, the spatial distribution of drought duration and frequency (identified by SPEI at 3-month timescale) values were analyzed and are shown in Figure 8b. The results show that the distribution of the long drought duration area was highly coincidental with the region where annual SPEI showed a decreasing trend (Figure 8a,b), with the longest drought duration reaching 22 months and being located mainly in southeastern Yunnan and southwestern Sichuan (Figure 8b). In addition, the drought duration values varied greatly from region to region, while the drought frequency in all

stations was roughly the same (Figure 8b). This result further emphasized that the drought duration played a dominant role in the regional difference of drought damage in southwest China.

For the least squares method, the regression equation established an R^2 of 0.35 and $p < 0.01$, which indicates that these regressions fit the drought duration well. As shown in Table 3, the standardized coefficients indicate that the precipitation and ET_0 were negative and positive, respectively, in relation to the drought duration, which indicates that both precipitation increases (decreases) and ET_0 decreases (increases) reduce (prolong) the drought duration. When comparing the relative contributions of precipitation and ET_0 to the drought duration, we found a larger absolute value for the contribution of ET_0 compared with the contribution of precipitation. This result indicates that the drought duration responses were more sensitive to ET_0 than to precipitation in Southwest China.

Table 3. Relative contribution of precipitation and ET_0 to the drought duration.

	Precipitation	ET_0	Longitude	Latitude
Standardized coefficient	−0.179	0.519	0.1243	−0.1381
Relative contribution	18.63	54.06	12.94	14.37

4. Discussion

4.1. Impacts of Climatic Driving Factors on the Variation in ET_0

As human activities continue to exacerbate climate change, the global water balance is believed to be changing significantly, and many climate effects have already been seen [50,51]. Because ET_0 plays an essential role in the hydrological cycle, numerous studies have focused on the spatial and temporal variations of ET_0 under global warming [24,52]. These studies have shown that in the long time series, a transformation from downward to upward in ET_0 has been detected in most parts of China, whereas the air temperature has continued to increase. This scenario accurately illustrates that the variation in ET_0 is affected by many factors and that each factor carries a different weight at a different time period. Therefore, exploring the effects of climatic variables on ET_0 will assist researchers in predicting the variations in ET_0 and elucidating its driving mechanisms in the context of climate change.

Solar radiation is the dominant source of energy on the land surface, and its variations at the earth surface have profound effects on the human and terrestrial environment. Estimates of solar radiation values by Tsun are widely accepted, and they compare well with measured values [53,54]. During the period from 1960 to 1990, trends in ET_0 showed continued and significant ($o < 0.01$) decreases but a slight increase after 1990 (Figure 2h). That increase was highly coincidental with findings from across the world indicating that global solar radiation had changed from dimming to brightening, with the transition occurring around the 1990s [55,56]. In addition, our results show, based on the partial correlation and multilinear regression analyses, that the changes in Tsun were the predominant factor controlling the variations in ET_0 in Southwest China. These results are consistent with many previous research studies in Southwest China [21,57,58]. However, the mechanism of Tsun change has been the topic of much debate. Among the proposed mechanisms, numerous studies have attributed the decrease in sunshine duration to an increase in cloud coverage [59,60]. This explanation seems to be untenable in Southwest China, where declining precipitation in this area has often been reported [61,62] and was also found in this study (Figure 2g). Conversely, aggregated aerosols and pollution, accompanied by rapid industrialization and urbanization, have been suggested as the predominant dimming factor in Southwest China [63,64]. It is worth noting that stations located around the major cities in Southwest China, such as in Chongqing, where the population density is higher and human activity is concentrated, have all shown significant decreases in Tsun. Consequently, we also

believe that anthropogenic activities do have a crucial impact on the changes in sunshine duration in Southwest China.

Relative humidity refers to the percentage of vapor pressure in the air in relation to the saturated vapor pressure at the same temperature. It is affected by factors such as the atmospheric circulation, cloud cover, precipitation, wind, and terrain. It also plays an important role in the changes in ET_0. Our results show a significant decreasing trend in relative humidity, especially after 2000 (Figure 2d), which is highly coincidental with the findings of Fan and Thomas [57]. A decrease in relative humidity reduces atmospheric vapor and accelerates the release of water vapor from the land surface. McCulley et al. [65] similarly concluded that a 10% decrease in relative humidity resulted in an average increase of 28.33 to 59.42% in ET_0. In addition, our results show that relative humidity is another major factor influencing ET_0 in Southwest China. In the spring and winter, variations in relative humidity even became the primary factor contributing to changes in ET_0 (Table 2). This finding is supported by Jiang et al. [66], who concluded that the decline in relative humidity in Southwest China has mainly resulted from a decrease in precipitation.

The air temperature (Tmean, Tmin, and Tmax) showed a considerable increasing trend over the entire study period (Figure 2a–c). However, this stable increase in temperature contributed little to changes in ET_0 when compared with other climatic driving factors. This may have been due to the relatively smaller change in magnitude during the study period. In the long run, even if the contribution rate of temperature was not high, the continued increase in temperature would have a huge cumulative impact on ET_0. Numerous studies have found that temperature changes are controlled by long-wave radiation, whose variations are closely linked to climatic factors such as precipitation, cloud cover, water vapor, wind speed, and their complex intersection [35,67]. Recently, however, the predominant reason given to explain global warming has been the increasing use of aerosols and the increase in greenhouse gas emissions caused by economic development and population growth [68–70]. In addition, our results show that the temperature increase was more apparent at higher altitudes than at lower ones; thus, the relatively high-contribution areas are located mainly at the higher altitudes (Figure 6a), which coincides with the finding of Li et al. [71]. It may be that the unique natural environment in high-altitude areas of Southwest China has caused these areas to become more sensitive to temperature changes. For example, Liu and Chen [72] deduced that the positive feedback from snow and ice albedo was an important factor influencing climate warming at higher altitudes. As the increase in temperature accelerates the melting of snow and ice, this in turn reduces the surface albedo in high-altitude areas, resulting in increased absorption of solar radiation on the land surface and further increasing the temperature. In addition, Duan and Wu [73] demonstrated that increasing and decreasing trends in low-level clouds during the nighttime and daytime, respectively, resulted in enhanced atmospheric counterradiation at night and more absorption of direct solar radiation in the daytime, eventually resulting in surface warming in the central and eastern Tibetan Plateau (including the high-altitude areas of Southwest China).

The wind speed showed a slightly decreasing trend in the 1960s, whereas a rapidly increasing step change was found around 1970, which then decreased considerably until 2000, and further showed a significant increase in recent years. Previous researchers have found the same trend [66,74]. Our results show that the wind speed was significantly ($p < 0.01$) decreased over the entire study period and had a relative low contribution to the variations in ET_0 at both the annual and seasonal timescales when compared with other climatic driving factors (Table 2). However, Middelkoop et al. [50] reported that a nonsignificant decline in wind speed was dominated by a significant decrease in ET_0 throughout the entire study period (1961–2016), the differences that existed from our study may have been due to differences in the study areas and methods of analysis. In addition, reasons for the decrease in wind speed have still been attributed to the effects of natural factors and human activities. For example, Zhang et al. [75] emphasized that large-scale unstable atmospheric circulation and regional warming were the main reasons for the weakening of wind speed in Southwest China. Guo et al. [76] and Yang et al. [77] found that a weakening of the lower tropospheric pressure-gradient force was the

primary cause of the decrease in observed surface winds in recent years. Anthropogenic activities, including plantations, air pollution, and especially rapid urbanization, are also considered to play an important role in decreasing the wind speed by increasing surface roughness [76,78]. However, in past decades, the fastest development of urbanization in Southwest China has been accompanied by an increase in wind speed. Therefore, we believe that changes in natural factors are the main driving force for the declining wind speed over the entire study period.

4.2. The Evaporation Paradox

The evaporation paradox has attracted the attention of many researchers since it was first introduced [10]. Several studies have attempted to explain what causes this paradoxical phenomenon, including the hydrologic cycle, decreasing sunlight, wind speed, or an increase in relative humidity [79]. However, the decrease in sunlight resulting from an increase in cloud aerosol concentration has been widely considered the primary cause [9]. In addition, the implications of the evaporation paradox have attracted considerable attention. A complementary hypothesis formulated by Brutsaert and Parlange [79] proposed that the increased terrestrial evaporation (i.e., an accelerated global hydrological cycle) would increase moisture in the air, thus reducing pan-evaporation. Therefore, it was commonly thought that the widely observed decline in ET_0 or pan-evaporation was decelerating the global terrestrial hydrological cycle, which was then expected to accelerate as global dimming moved to brightening [80,81].

In China, Liu et al. (2004) found that pan-evaporation decreased from 1955 to 2000, which they attributed to a decrease in solar irradiance [82]. However, Cong et al. [83] found an increasing trend in ET_0 from 1986 to 2005 for the entire period, which indicates that the evaporation paradox had disappeared in China as a whole. Regarding whether this phenomenon still exists in Southwest China, our results show that the climatic warming trend was obvious over the past 59 years from 1960 to 2018 in Southwest China (Figure 2a). Thus, the evaporation paradox existed before the 2000s because the ET_0 showed a continuous decrease. However, after the 2000s, the positive effect of an increase in air temperature on ET_0 exceeded the negative effect on ET_0 by decreasing the sunshine duration and wind speed. Especially for the study period from 1960 to 2018, the ET_0 also showed a nonsignificant ($p > 0.05$) increase. This result was highly consistent with those obtained by Li et al. [14] and Jiang et al. [66]. Consequently, we can conclude that at present, the evaporation paradox has disappeared in Southwest China as global warming continues.

4.3. Agricultural Water Management Under a Background of Increasing ET_0

Any changes in ET_0 rates will have an impact on the terrestrial ecosystem. Agriculture, in particular, involves a major consumptive use of irrigation water and precipitation on agricultural land. The attempt to improve the efficiency of water use must be based on reliable estimates of ET_0.

Our results show that the trend in ET_0 altered from significantly decreasing from 1960 to 2000 to increasing after 2000, which indicates that the continuous increase in temperature and decrease in relative humidity has offset the impact of the significant decrease in Tsun and wind speed, dominating the change in ET_0 in Southwest China. For a long period to come, what is certain is that the temperature will continue to increase because of an increasing concentration of greenhouse gases in the atmosphere [84]. Consequently, the contribution of the temperature rise to changes in ET_0 will be further strengthened. In other words, ET_0 will most likely maintain an increasing trend over the period ahead. This perspective is supported by Wang et al. [85], who concluded that the increase in potential evapotranspiration, attributable to the joint effects of increased temperature and surface net radiation and decreased relative humidity, will overwhelm the entire region throughout the 21st century. The consequence of the continued increase in ET_0 is that Southwest China will face a great risk of drought, because we have found that the contribution of changes in ET_0 to drought is equal to or even greater than the contribution of changes in precipitation. Wang et al. [85], who also

reached the same conclusion, emphasized that the enhancement of potential evapotranspiration will outweigh that of precipitation, particularly under Representative Concentration Pathway 8.5, resulting in intensified drought.

Because water availability and accessibility are the most significant constraining factors for crop production, agriculture is the economic sector primarily affected by drought. Therefore, addressing the issues of agricultural water shortage and guaranteed food production is crucial in Southwest China. To achieve this, we quantitatively assessed the temporal and spatial distribution of agricultural drought risks in Southwest China in our previous study [28]. We also proposed strategies to mitigate the risk of agricultural drought according to local soil, climatic, topographic, irrigation, economic, and educational conditions.

Additionally, China has experienced rapid urbanization and industrialization in recent decades, leading to increased pressure to shift water out of agriculture to supply drinking water to growing cities. Yan et al. [86] found that the share of agricultural water use in China declined from 73 to 63% and that the urbanization rate increased from 28 to 51% from 1993 to 2011. Therefore, how to promote water resources so they flow healthily and successfully from rural to urban areas or from agriculture to industry is also of great significance for improving the ability of Southwest China to cope with agricultural water scarcity, or even agricultural droughts. For this purpose, we think other appropriate measures, including those of a financial nature, are required to support farmers, given that primarily, farmers' incomes may be drastically reduced. Therefore, we suggest that the government manages water resources by articulating water use rights and establishing a water market, which will permit the purchase and sale of water across sectors, districts, and time. In the process, water users should consider the comprehensive opportunity cost of water, including its value in alternative uses. This will provide incentives to economize water resources and gain additional income. Furthermore, water treatment and reuse can provide alternative water resources and thus ease the contradiction between urban and rural water use. As Yi et al. [87] pointed out, 80% of the water consumed in an urban area ends up in the wastewater stream, and 70% of it may be reclaimed if the wastewater is collected and treated. However, most areas of China are still undeveloped, mainly because of a lack of investment, so induced wastewater treatment and reuse ratios are relatively low (70.2% and 9.2% in 2008, respectively) compared with those in developed countries (more than 80% and 70%, respectively) [88]. Therefore, the administration of Southwest China will be expected to increase its investment in water reuse research and to focus on sustainable regional water resource management, while regarding water reclamation, recycling, and reuse as key components of the regional water strategy.

5. Conclusions

Numerous researchers have pointed out that trends in ET_0 have changed greatly as climate change has been intensified. In the present study, we selected Southwest China as a typical region and investigated the spatiotemporal variation in ET_0, the trends in ET_0, the contributions of four climatic driving factors to trends in ET_0, and the impact of shifts in ET_0 on the drought duration based on data from 1960 to 2018 from 79 meteorological stations.

The annual ET_0 reflected a significant decrease by 14.1 mm/decade from 1960 to 2000, but an obvious increase after 2000. Especially during the period from 2001 to 2013, the annual ET_0 increased significantly, by 51.3 mm per decade. Over the entire study period, the annual ET_0 (average of all stations) showed a statistically nonsignificant increase of 9.7 mm per decade, with the stations that showed significant increases located mainly in Yunnan and northern Sichuan. The degree of correlation between ET_0 and other climatic driving factors during this period decreased in the order of Tsun, U2, relative humidity, and Tmean, with the specific correlation coefficients of 0.95, 0.9, −0.84, and 0.83, respectively. Additionally, Tsun was the most important factor dominating the changes in ET_0 for all of Southwest China at the annual timescales. The dominant factors showed some differences at the seasonal timescales, with Tsun also playing a dominant role in the summer and

autumn, but relative humidity replacing Tsun as the dominant factor in the spring and winter. It is important to note that ET_0 made a greater contribution to the drought duration than did precipitation. Under the background of global warming, the continued increasing in ET_0 will further exacerbate the drought problem in southwest China.

Author Contributions: Z.Z. and W.W. designed the research and performed the analysis, and Z.Z. wrote the first draft. Z.Z., W.W., Z.L., and Y.Z. reviewed and edited the draft. M.H. and H.H. collected the data.

Conflicts of Interest: The authors declare no conflict of interest.

References

1. Barnett, T.P.; Adam, J.C.; Lettenmaier, D.P. Potential impacts of a warming climate on water availability in snow-dominated regions. *Nature* **2005**, *438*, 303–309. [CrossRef] [PubMed]
2. Menzel, L.; Burger, G. Climate change scenarios and runoff response in the Mulde catchment (Southern Elbe, Germany). *J. Hydrol.* **2002**, *267*, 53–64. [CrossRef]
3. Xu, C.Y.; Singh, V.P. Evaluation of three complementary relationship evapotranspiration models by water balance approach to estimate actual regional evapotranspiration in different climatic regions. *J. Hydrol.* **2005**, *308*, 105–121. [CrossRef]
4. Chahine, M.T. The hydrological cycle and its influence on climate. *Nature* **1992**, *359*, 373–380. [CrossRef]
5. Allen, R.G.; Pereira, L.S.; Raes, D.; Smith, M. *Crop Evapotranspiration—Guidelines for Computing Crop Water Requirements—FAO Irrigation and Drainage Paper 56*; Fao: Rome, Italy, 1998; Volume 300, p. D05109.
6. Zhang, X.; Ren, Y.; Yin, Z.-Y.; Lin, Z.; Zheng, D. Spatial and temporal variation patterns of reference evapotranspiration across the Qinghai-Tibetan Plateau during 1971–2004. *J. Geophys. Res. Atmos.* **2009**, *114*. [CrossRef]
7. Han, J.; Zhao, Y.; Wang, J.; Zhang, B.; Zhu, Y.; Jiang, S.; Wang, L. Effects of different land use types on potential evapotranspiration in the Beijing-Tianjin-Hebei region, North China. *J. Geogr. Sci.* **2019**, *29*, 922–934. [CrossRef]
8. Solomon, S.; Qin, D.; Manning, M.; Averyt, K.; Marquis, M. *Climate Change 2007—The Physical Science Basis: Working Group I Contribution to the Fourth Assessment Report of the IPCC*; Cambridge University Press: Cambridge, UK, 2007; Volume 4.
9. Roderick, M.L.; Farquhar, G.D. The cause of decreased pan evaporation over the past 50 years. *Science* **2002**, *298*, 1410–1411.
10. Peterson, T.C.; Golubev, V.S.; Groisman, P.Y. Evaporation losing its strength. *Nature* **1995**, *377*, 687–688. [CrossRef]
11. Tabari, H.; Aeini, A.; Talaee, P.H.; Some'e, B.S. Spatial distribution and temporal variation of reference evapotranspiration in arid and semi-arid regions of Iran. *Hydrol. Process.* **2012**, *26*, 500–512. [CrossRef]
12. Bandyopadhyay, A.; Bhadra, A.; Raghuwanshi, N.S.; Singh, R. Temporal Trends in Estimates of Reference Evapotranspiration over India. *J. Hydrol. Eng.* **2009**, *14*, 508–515. [CrossRef]
13. Burn, D.H.; Hesch, N.M. Trends in evaporation for the Canadian prairies. *J. Hydrol.* **2007**, *336*, 61–73. [CrossRef]
14. Li, Z.; Feng, Q.; Wei, L.; Wang, T.; Gao, Y.; Wang, Y.; Cheng, A.; Li, J.; Liu, L. Spatial and temporal trend of potential evapotranspiration and related driving forces in Southwestern China, during 1961–2009. *Quat. Int.* **2014**, *336*, 127–144. [CrossRef]
15. Xu, L.; Shi, Z.; Wang, Y.; Zhang, S.; Chu, X.; Yu, P.; Xiong, W.; Zuo, H.; Wang, Y. Spatiotemporal variation and driving forces of reference evapotranspiration in Jing River Basin, northwest China. *Hydrol. Process.* **2015**, *29*, 4846–4862. [CrossRef]
16. Chen, S.; Liu, Y.; Thomas, A. Climatic change on the Tibetan Plateau: Potential evapotranspiration trends from 1961–2000. *Clim. Chang.* **2006**, *76*, 291–319. [CrossRef]
17. Ning, T.; Li, Z.; Liu, W.; Han, X. Evolution of potential evapotranspiration in the northern Loess Plateau of China: Recent trends and climatic drivers. *Int. J. Climatol.* **2016**, *36*, 4019–4028. [CrossRef]

18. Wang, Q.; Wang, J.; Zhao, Y.; Li, H.; Zhai, J.; Yu, Z.; Zhang, S. Reference evapotranspiration trends from 1980 to 2012 and their attribution to meteorological drivers in the three-river source region, China. *Int. J. Climatol.* **2016**, *36*, 3759–3769. [CrossRef]

19. Wang, W.; Shao, Q.; Peng, S.; Xing, W.; Yang, T.; Luo, Y.; Yong, B.; Xu, J. Reference evapotranspiration change and the causes across the Yellow River Basin during 1957–2008 and their spatial and seasonal differences. *Water Resour. Res.* **2012**, *48*. [CrossRef]

20. Tang, B.; Tong, L.; Kang, S.; Zhang, L. Impacts of climate variability on reference evapotranspiration over 58 years in the Haihe river basin of north China. *Agric. Water Manag.* **2011**, *98*, 1660–1670. [CrossRef]

21. Yin, Y.; Wu, S.; Dai, E. Determining factors in potential evapotranspiration changes over China in the period 1971–2008. *Chin. Sci. Bull.* **2010**, *55*, 3329–3337. [CrossRef]

22. Wang, X.-M.; Liu, H.-J.; Zhang, L.-W.; Zhang, R.-H. Climate change trend and its effects on reference evapotranspiration at Linhe Station, Hetao Irrigation District. *Water Sci. Eng.* **2014**, *7*, 250–266. [CrossRef]

23. Li, Z.; Zheng, F.-L.; Liu, W.-Z. Spatiotemporal characteristics of reference evapotranspiration during 1961–2009 and its projected changes during 2011–2099 on the Loess Plateau of China. *Agric. For. Meteorol.* **2012**, *154*, 147–155. [CrossRef]

24. Han, J.; Wang, J.; Zhao, Y.; Wang, Q.; Zhang, B.; Li, H.; Zhai, J. Spatio-temporal variation of potential evapotranspiration and climatic drivers in the Jing-Jin-Ji region, North China. *Agric. For. Meteorol.* **2018**, *256*, 75–83. [CrossRef]

25. Li, Y.; Liang, K.; Bai, P.; Feng, A.; Liu, L.; Dong, G. The spatiotemporal variation of reference evapotranspiration and the contribution of its climatic factors in the Loess Plateau, China. *Environ. Earth Sci.* **2016**, *75*. [CrossRef]

26. Zhang, D.; Hong, H.; Zhang, Q.; Nie, R. Effects of climatic variation on pan-evaporation in the Poyang Lake Basin, China. *Clim. Res.* **2014**, *61*, 29–40. [CrossRef]

27. Zhang, Y.; Peña-Arancibia, J.L.; McVicar, T.R.; Chiew, F.H.; Vaze, J.; Liu, C.; Lu, X.; Zheng, H.; Wang, Y.; Liu, Y.Y. Multi-decadal trends in global terrestrial evapotranspiration and its components. *Sci. Rep.* **2016**, *6*, 19124. [CrossRef]

28. Zeng, Z.; Wu, W.; Li, Z.; Zhou, Y.; Guo, Y.; Huang, H.J.W. Agricultural Drought Risk Assessment in Southwest China. *Water* **2019**, *11*, 1064. [CrossRef]

29. Milly, P.C.D.; Wetherald, R.T.; Dunne, K.A.; Delworth, T.L. Increasing risk of great floods in a changing climate. *Nature* **2002**, *415*, 514–517. [CrossRef]

30. Palmer, T.N.; Ralsanen, J. Quantifying the risk of extreme seasonal precipitation events in a changing climate. *Nature* **2002**, *415*, 512–514. [CrossRef]

31. Dai, A. Increasing drought under global warming in observations and models. *Nat. Clim. Chang.* **2013**, *3*, 171. [CrossRef]

32. Livada, I.; Assimakopoulos, V.D. Spatial and temporal analysis of drought in Greece using the Standardized Precipitation Index (SPI). *Theor. Appl. Climatol.* **2007**, *89*, 143–153. [CrossRef]

33. Piccarreta, M.; Capolongo, D.; Boenzi, F. Trend analysis of precipitation and drought in Basilicata from 1923 to 2000 within a southern Italy context. *Int. J. Climatol.* **2004**, *24*, 907–922. [CrossRef]

34. Luo, L.; Apps, D.; Arcand, S.; Xu, H.; Pan, M.; Hoerling, M. Contribution of temperature and precipitation anomalies to the California drought during 2012–2015. *Geophys. Res. Lett.* **2017**, *44*, 3184–3192. [CrossRef]

35. Sun, S.; Chen, H.; Ju, W.; Wang, G.; Sun, G.; Huang, J.; Ma, H.; Gao, C.; Hua, W.; Yan, G. On the coupling between precipitation and potential evapotranspiration: Contributions to decadal drought anomalies in the Southwest China. *Clim. Dyn.* **2017**, *48*, 3779–3797. [CrossRef]

36. Sun, S.; Chen, H.; Wang, G.; Li, J.; Mu, M.; Yan, G.; Xu, B.; Huang, J.; Wang, J.; Zhang, F.; et al. Shift in potential evapotranspiration and its implications for dryness/wetness over Southwest China. *J. Geophys. Res. Atmos.* **2016**, *121*, 9342–9355. [CrossRef]

37. Yu, M.; Li, Q.; Hayes, M.J.; Svoboda, M.D.; Heim, R.R. Are droughts becoming more frequent or severe in China based on the standardized precipitation evapotranspiration index: 1951–2010? *Int. J. Climatol.* **2014**, *34*, 545–558. [CrossRef]

38. Zhang, L.; Xiao, J.; Li, J.; Wang, K.; Lei, L.; Guo, H. The 2010 spring drought reduced primary productivity in southwestern China. *Environ. Res. Lett.* **2012**, *7*, 045706. [CrossRef]

39. Zhu, Z.L.; Zhao, X.J.; Wang, C.T.; Hou, L.C. The Rules of drought and the development of water-saving agriculture in southwest China. *Ecol. Environ.* **2006**, *15*, 876–880.

40. McEvoy, D.J.; Huntington, J.L.; Mejia, J.F.; Hobbins, M.T. Improved seasonal drought forecasts using reference evapotranspiration anomalies. *Geophys. Res. Lett.* **2016**, *43*, 377–385. [CrossRef]

41. Qin, N.; Chen, X.; Fu, G.; Zhai, J.; Xue, X. Precipitation and temperature trends for the Southwest China: 1960–2007. *Hydrol. Process.* **2010**, *24*, 3733–3744. [CrossRef]

42. Kendall, M. *Rank Correlation Methods*; Charles Griffin: London, UK, 1975.

43. Mann, H.B. Nonparametric tests against trend. *Econom. J. Econom. Soc.* **1945**, *13*, 245–259. [CrossRef]

44. Gocic, M.; Trajkovic, S. Analysis of changes in meteorological variables using Mann-Kendall and Sen's slope estimator statistical tests in Serbia. *Glob. Planet. Chang.* **2013**, *100*, 172–182. [CrossRef]

45. Umar, D.U.A.; Ramli, M.F.; Aris, A.Z.; Jamil, N.R.; Abdulkareem, J.H. Runoff irregularities, trends, and variations in tropical semi-arid river catchment. *J. Hydrol. Reg. Stud.* **2018**, *19*, 335–348. [CrossRef]

46. He, D.; Liu, Y.; Pan, Z.; An, P.; Wang, L.; Dong, Z.; Zhang, J.; Pan, X.; Zhao, P. Climate change and its effect on reference crop evapotranspiration in central and western Inner Mongolia during 1961–2009. *Front. Earth Sci.* **2013**, *7*, 417–428. [CrossRef]

47. Gao, G.; Chen, D.; Ren, G.; Chen, Y.; Liao, Y. Spatial and temporal variations and controlling factors of potential evapotranspiration in China: 1956–2000. *J. Geogr. Sci.* **2006**, *16*, 3–12. [CrossRef]

48. Vicente-Serrano, S.M.; Begueria, S.; Lopez-Moreno, J.I. A Multiscalar Drought Index Sensitive to Global Warming: The Standardized Precipitation Evapotranspiration Index. *J. Clim.* **2010**, *23*, 1696–1718. [CrossRef]

49. Ji, L.; Peters, A.J. Assessing vegetation response to drought in the northern Great Plains using vegetation and drought indices. *Remote Sens. Environ.* **2003**, *87*, 85–98. [CrossRef]

50. Middelkoop, H.; Daamen, K.; Gellens, D.; Grabs, W.; Kwadijk, J.C.J.; Lang, H.; Parmet, B.; Schadler, B.; Schulla, J.; Wilke, K. Impact of climate change on hydrological regimes and water resources management in the rhine basin. *Clim. Chang.* **2001**, *49*, 105–128. [CrossRef]

51. Wang, G.; Xia, J.; Chen, J. Quantification of effects of climate variations and human activities on runoff by a monthly water balance model: A case study of the Chaobai River basin in northern China. *Water Resour. Res.* **2009**, *45*. [CrossRef]

52. Zhang, D.; Liu, X.; Hong, H. Assessing the effect of climate change on reference evapotranspiration in China. *Stoch. Environ. Res. Risk Assess.* **2013**, *27*, 1871–1881. [CrossRef]

53. Bakirci, K. Correlations for estimation of daily global solar radiation with hours of bright sunshine in Turkey. *Energy* **2009**, *34*, 485–501. [CrossRef]

54. Almorox, J.; Hontoria, C. Global solar radiation estimation using sunshine duration in Spain. *Energy Convers. Manag.* **2004**, *45*, 1529–1535. [CrossRef]

55. Wild, M.; Gilgen, H.; Roesch, A.; Ohmura, A.; Long, C.N.; Dutton, E.G.; Forgan, B.; Kallis, A.; Russak, V.; Tsvetkov, A. From dimming to brightening: Decadal changes in solar radiation at Earth's surface. *Science* **2005**, *308*, 847–850. [CrossRef] [PubMed]

56. Ohmura, A. Observed decadal variations in surface solar radiation and their causes. *J. Geophys. Res. Atmos.* **2009**, *114*. [CrossRef]

57. Fan, Z.; Thomas, A. Spatiotemporal variability of reference evapotranspiration and its contributing climatic factors in Yunnan Province, SW China, 1961–2004. *Clim. Chang.* **2013**, *116*, 309–325. [CrossRef]

58. Sun, S.; Chen, H.; Sun, G.; Ju, W.; Wang, G.; Li, X.; Yan, G.; Gao, C.; Huang, J.; Zhang, F. Attributing the changes in reference evapotranspiration in Southwestern China using a new separation method. *J. Hydrometeorol.* **2017**, *18*, 777–798. [CrossRef]

59. Dai, A.; Karl, T.R.; Sun, B.; Trenberth, K.E. Recent trends in cloudiness over the United States—A tale of monitoring inadequacies. *Bull. Am. Meteorol. Soc.* **2006**, *87*, 597–606. [CrossRef]

60. Xia, X. Spatiotemporal changes in sunshine duration and cloud amount as well as their relationship in China during 1954–2005. *J. Geophys. Res. Atmos.* **2010**, *115*. [CrossRef]

61. Zhang, Q.; Li, Y. Climatic Variation of Rainfall and Rain Day in Southwest China for Last 48 Years. *Plateau Meteorol.* **2014**, *33*, 372–383.

62. Wang, S.; Jiao, S.; Xin, H. Spatio-temporal characteristics of temperature and precipitation in Sichuan Province, Southwestern China, 1960–2009. *Quat. Int.* **2013**, *286*, 103–115. [CrossRef]

63. Kaiser, D.P.; Qian, Y. Decreasing trends in sunshine duration over China for 1954-1998: Indication of increased haze pollution? *Geophys. Res. Lett.* **2002**, *29*, 38-1–38-4. [CrossRef]

64. Qian, Y.; Kaiser, D.P.; Leung, L.R.; Xu, M. More frequent cloud-free sky and less surface solar radiation in China from 1955 to 2000. *Geophys. Res. Lett.* **2006**, *33*. [CrossRef]

65. McCulley, J.P.; Aronowicz, J.D.; Uchiyama, E.; Shine, W.E.; Butovich, I.A. Correlations in a change in aqueous tear evaporation with a change in relative humidity and the impact. *Am. J. Ophthalmol.* **2006**, *141*, 758–760. [CrossRef] [PubMed]

66. Jiang, S.; Liang, C.; Cui, N.; Zhao, L.; Du, T.; Hu, X.; Feng, Y.; Guan, J.; Feng, Y. Impacts of climatic variables on reference evapotranspiration during growing season in Southwest China. *Agric. Water Manag.* **2019**, *216*, 365–378. [CrossRef]

67. Loginov, S.V.; Ippolitov, I.I.; Kharyutkina, E.V. The relationship of surface air temperature, heat balance at the surface, and radiative balance at the top of atmosphere over the Asian territory of Russia using reanalysis and remote-sensing data. *Int. J. Remote Sens.* **2014**, *35*, 5878–5898. [CrossRef]

68. Kerr, R.A. Climate change. It's official: Humans are behind most of global warming. *Science (N. Y.)* **2001**, *291*, 566. [CrossRef]

69. Gleckler, P.J.; Santer, B.D.; Domingues, C.M.; Pierce, D.W.; Barnett, T.P.; Church, J.A.; Taylor, K.E.; AchutaRao, K.M.; Boyer, T.P.; Ishii, M.; et al. Human-induced global ocean warming on multidecadal timescales. *Nat. Clim. Chang.* **2012**, *2*, 524–529. [CrossRef]

70. Akorede, M.F.; Hizam, H.; Ab Kadir, M.Z.A.; Aris, I.; Buba, S.D. Mitigating the anthropogenic global warming in the electric power industry. *Renew. Sustain. Energy Rev.* **2012**, *16*, 2747–2761. [CrossRef]

71. Li, Z.; He, Y.; An, W.; Song, L.; Zhang, W.; Catto, N.; Wang, Y.; Wang, S.; Liu, H.; Cao, W.; et al. Climate and glacier change in southwestern China during the past several decades. *Environ. Res. Lett.* **2011**, *6*, 045404. [CrossRef]

72. Liu, X.D.; Chen, B.D. Climatic warming in the Tibetan Plateau during recent decades. *Int. J. Climatol.* **2000**, *20*, 1729–1742. [CrossRef]

73. Duan, A.; Wu, G. Change of cloud amount and the climate warming on the Tibetan Plateau. *Geophys. Res. Lett.* **2006**, *33*. [CrossRef]

74. Fu, G.; Yu, J.; Zhang, Y.; Hu, S.; Ouyang, R.; Liu, W. Temporal variation of wind speed in China for 1961–2007. *Theor. Appl. Climatol.* **2011**, *104*, 313–324. [CrossRef]

75. Zhang, Z.; Yang, Y.; Zhang, X.; Chen, Z. Wind speed changes and its influencing factors in Southwestern China. *Acta Ecol. Sin.* **2014**, *34*, 471–481.

76. Guo, H.; Xu, M.; Hu, Q. Changes in near-surface wind speed in China: 1969–2005. *Int. J. Climatol.* **2011**, *31*, 349–358. [CrossRef]

77. Yang, X.; Li, Z.; Feng, Q.; He, Y.; An, W.; Zhang, W.; Cao, W.; Yu, T.; Wang, Y.; Theakstone, W.H. The decreasing wind speed in southwestern China during 1969-2009, and possible causes. *Quat. Int.* **2012**, *263*, 71–84. [CrossRef]

78. Li, Z.; Yan, Z.; Tu, K.; Liu, W.; Wang, Y. Changes in Wind Speed and Extremes in Beijing during 1960–2008 Based on Homogenized Observations. *Adv. Atmos. Sci.* **2011**, *28*, 408–420. [CrossRef]

79. Brutsaert, W.; Parlange, M.B. Hydrologic cycle explains the evaporation paradox. *Nature* **1998**, *396*, 30. [CrossRef]

80. Wild, M. Global dimming and brightening: A review. *J. Geophys. Res. Atmos.* **2009**, *114*. [CrossRef]

81. Wang, T.; Zhang, J.; Sun, F.; Liu, W. Pan evaporation paradox and evaporative demand from the past to the future over China: A review. *Wiley Interdiscip. Rev. Water* **2017**, *4*. [CrossRef]

82. Liu, B.H.; Xu, M.; Henderson, M.; Gong, W.G. A spatial analysis of pan evaporation trends in China, 1955–2000. *J. Geophys. Res. Atmos.* **2004**, *109*, e1207. [CrossRef]

83. Cong, Z.T.; Yang, D.W.; Ni, G.H. Does evaporation paradox exist in China? *Hydrol. Earth Syst. Sci.* **2009**, *13*, 357–366. [CrossRef]

84. Wen, Q.H.; Zhang, X.; Xu, Y.; Wang, B. Detecting human influence on extreme temperatures in China. *Geophys. Res. Lett.* **2013**, *40*, 1171–1176. [CrossRef]

85. Wang, L.; Chen, W.; Zhou, W. Assessment of Future Drought in Southwest China Based on CMIP5 Multimodel Projections. *Adv. Atmos. Sci.* **2014**, *31*, 1035–1050. [CrossRef]

86. Yan, T.; Wang, J.; Huang, J. Urbanization, agricultural water use, and regional and national crop production in China. *Ecol. Model.* **2015**, *318*, 226–235. [CrossRef]

87. Yi, L.; Jiao, W.; Chen, X.; Chen, W. An overview of reclaimed water reuse in China. *J. Environ. Sci.* **2011**, *23*, 1585–1593. [CrossRef]

88.   Bao, C.; Fang, C.-L. Water Resources Flows Related to Urbanization in China: Challenges and Perspectives for Water Management and Urban Development. *Water Resour. Manag.* **2012**, *26*, 531–552. [CrossRef]